# On the Stability of the Flow through a Spherical Bulge in a 90º Asymmetrical Bend

J. M. M. Sousa[1]

## Summary

Time-dependent numerical simulations of the flow through a spherical bulge in a 90° asymmetrical bend have been performed for Reynolds numbers in the range 100-400. Present results have shown that the flow reaches asymptotically steady solutions for Reynolds numbers up to 300, whereas a value of 400 for this parameter leads to unsteadiness. The computed flow behavior at this higher Reynolds number has shown to be characterized by long transients of small-amplitude, irregular oscillations, which are suddenly disrupted by short periods of large-amplitude bursts.

## Introduction

It is well known that impinging jets and flows in cavity-type geometries are prone to exhibit self-sustained oscillations [1]. Both periodic [2] and aperiodic cavities [3] have been shown to develop an oscillatory flow behavior when a certain value of the Reynolds number is exceeded. On the other hand, the classical example of a diverging channel (with the sudden expansion as a limit case) is also known to present hydrodynamic instabilities that may lead to different types of bifurcations [4]. Symmetry-breaking of the flow, giving rise to non-unique solutions, arise in such flows through a supercritical pitchfork bifurcation [5]. In addition, transition from a steady solution to periodic flow has been reported to occur in channels with expanded sections as a consequence of a Hopf bifurcation [6].

The flow through a bulge in a bend belongs to the class of flows in cavity-type geometries, displaying a three-dimensional, gradual expansion and contraction of the flow through the main channel. Furthermore, the confined jet produced at the entrance of the bulge impinges at the opposite surface, thus providing an additional source of instability in this flow. In the present case, a spherical bulge with a diameter ratio of 16/9 was considered. The 90° bend is asymmetric because the outlet channel has a smaller diameter than the inlet duct and its axis is displaced by a small amount along the main channel direction. The diameter ratio between the two ducts is 35/54 and the ratio of the axis displacement to the main channel diameter is 1/15.

The practical interest of this work can be found in the fields of *in vitro* studies of hemodynamics and pharmacokinetics. Concerning the first application, the relevance of this geometry arises from the fact that it can be seen as a simplified model of a saccular

[1] Instituto Superior Técnico, Technical University of Lisbon, Mechanical Engineering Department, Av. Rovisco Pais, 1049-001 Lisboa, Portugal

aneurysm. Although a Newtonian fluid was considered here and the effects of compliant walls and pulsatile inlet flow were not taken into account, the numerical simulations carried out for the present investigation are in the same range of Reynolds number as the blood flow in intra-cranial arteries [7]. Studies of hydrodynamic stability [8] and chaotic mixing [9] in aneurysm models have been reported in the literature, demonstrating the importance of these problems. The second application results from the observation that the present geometry faithfully reproduces the throat section of a standard apparatus used in the pharmacological assessment of the performance of dry powder inhalers. In this case, it can be is easily demonstrated that the dynamics of the gas flow has a significant impact on the deposition characteristics of an aerosol in such device.

## Numerical Procedures

The mass and momentum conservation equations governing the unsteady flow of an incompressible, Newtonian fluid (1)-(2) were solved numerically. Denoting the fluid density by $\rho$, the velocity vector by $\boldsymbol{v}$ and the stress tensor by $\boldsymbol{\tau}$, these equations can be written in vector form as

$$\nabla \cdot \left( \rho \boldsymbol{v} \right) = 0 \,, \tag{1}$$

$$\frac{\partial}{\partial t}\left( \rho \boldsymbol{v} \right) + \nabla \cdot \left( \rho \boldsymbol{v} : \boldsymbol{v} - \boldsymbol{\tau} \right) = 0 \,. \tag{2}$$

Steady and time-dependent flow solutions have been obtained employing the finite-volume method to discretize the equations on a structured, non-orthogonal, non-staggered grid system. The numerical method is second-order accurate in space and in time, using Crank-Nicholson and Adams-Bashforth time-stepping procedures to advance diffusion and convective terms in time, respectively. Additional details regarding the numerical method were given by Pereira and Sousa [10].

The boundaries defining the geometry of physical domain where numerical solutions of (1)-(2) have been sought were obtained from digital images of cut planes of a glass model produced by laser light sheet illumination. A hybrid elliptic-algebraic procedure has been adopted for the generation of the numerical grid, aiming to discretize the physical domain in finite volumes. Two different levels of discretization have been considered: coarse ($32 \times 32 \times 70$ grid nodes) and fine ($62 \times 62 \times 138$ grid nodes). Figure 1 illustrates both the numerical grid and the geometry of the physical domain. No-slip boundary conditions have been applied to all domain surfaces, with the exception of the inlet and outlet sections. At the inlet, a uniform, time-independent $w$-velocity profile was prescribed. The velocity magnitude was adjusted from case to case according to the desired value of the Reynolds number $Re$ (based on the inlet velocity and diameter) for the simulation. On the other hand, a Sommerfeld radiation condition was implemented at the outlet section, aiming to minimize undesired wave reflections from this boundary.

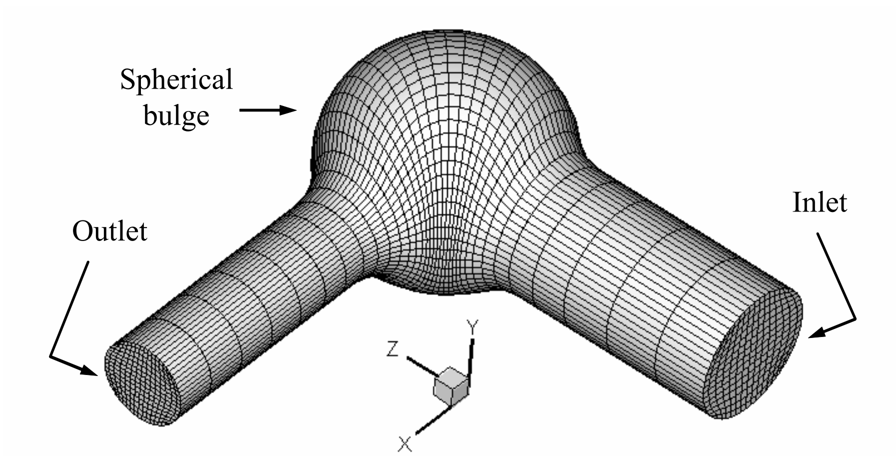


Figure 1. Geometry of the physical domain and numerical grid (only odd lines of the coarse discretization are shown for clarity).

## Results and Discussion

Due to the long time required to carry out the time-dependent numerical simulations, the flow solutions presented and discussed in this section have been obtained employing the coarse grid only. Numerical grid independence is currently under investigation.

Initial simulations carried out for increasing values of the Reynolds number in the range 100-300 yielded asymptotically steady solutions of the flow. These are sketched in Figure 2, in terms of in-plane velocity vectors, for the *y-z* meridional plane of the spherical bulge. The figure portrays purely symmetrical flow patterns with increasing complexity. The dimension of the main recirculations shown in the figure is also seen increasing with the Reynolds number.

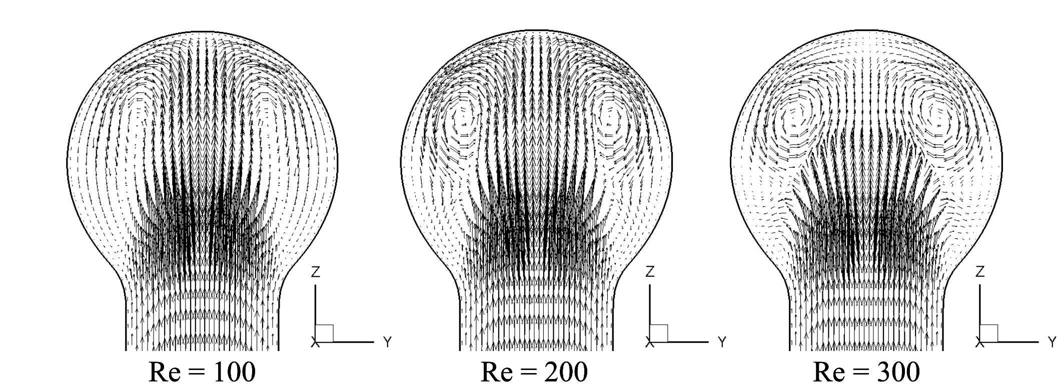


Figure 2. Steady flow patterns at the *y-z* meridional plane of the spherical bulge as a function of Reynolds number (velocity vectors have been scaled).

An additional simulation was performed for $Re = 400$. However, in this case, the flow did not reach a steady state. In contradistinction, the *v*-velocity trace at a monitor point located in the *x-z* meridional plane of the spherical bulge displayed long transients of small-amplitude, irregular oscillations, which were suddenly disrupted by short periods of large-amplitude bursts, as shown in Figure 3. In addition, this figure proves that the symmetry of the flow was broken.

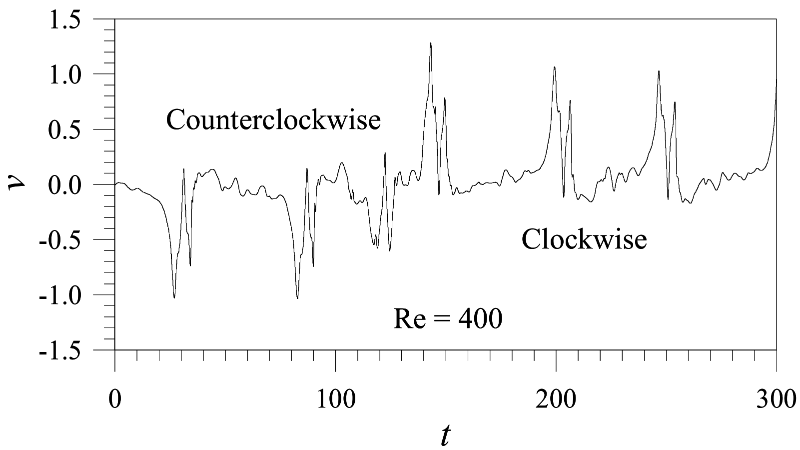


Figure 3. Time trace of the *v*-velocity component at a monitor point located in the *x-z* meridional plane of the spherical bulge for $Re = 400$.

It is undeniable that the intermittence illustrated in Figure 3 exhibits a certain degree of organization. Namely, the bursts occur at an approximately constant non-dimensional frequency $\omega = 0.018$. There is an obvious exception to this behavior, which took place at $t \approx 120$. This seemed to correspond to a crisis, leading to a change in the sense of rotation of the larger vortex associated to bursting events. Figure 4 substantiates this assertion by portraying two instantaneous flow maps recorded at equivalent stages of bursts occurring before and after the crisis. Figure 5 depicts the differences between instantaneous flow patterns associated to the regime of small-amplitude oscillations and representative of a bursting event, at the *x-z* meridional plane.

The observed behavior presents a few similarities with the transition mechanisms described by the so-called Pomeau-Manneville model [11]. However, in this case, prior to the establishment of a regime of intermittent chaotic motion, a periodic state (arising via Hopf bifurcation) is expected to occur. This regime may lie somewhere in between $Re = 300$ and $Re = 400$. Additional numerical simulations are required to investigate this issue as well as the grid independence of the present solutions. However, it must be mentioned that symmetry-breaking of the flow in the bulge and the low-frequency component $(\omega = 0.016)$ have also been observed in the course of an experimental investigation [12] of this flow for $Re = 3000$.

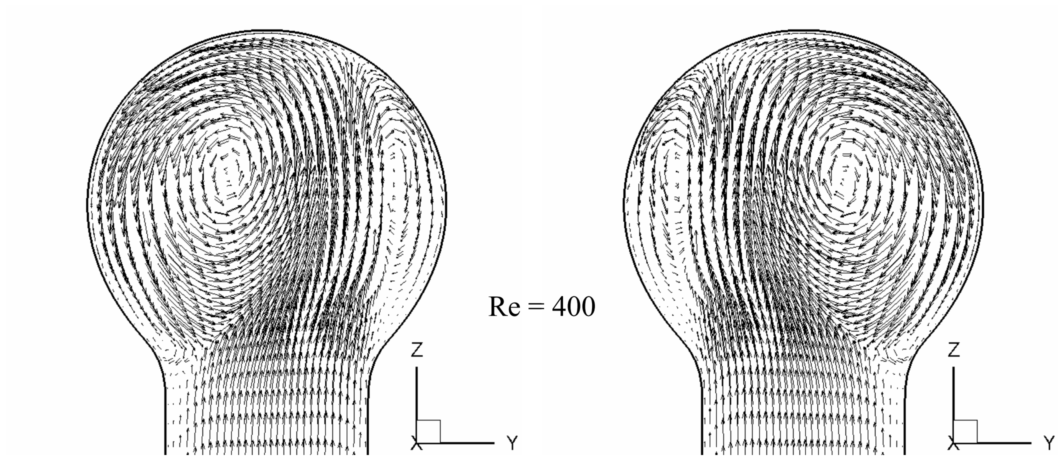


Figure 4. Instantaneous flow maps at the *y*-*z* meridional plane of the spherical bulge for $Re = 400$, before the crisis (left) and after the crisis (right).

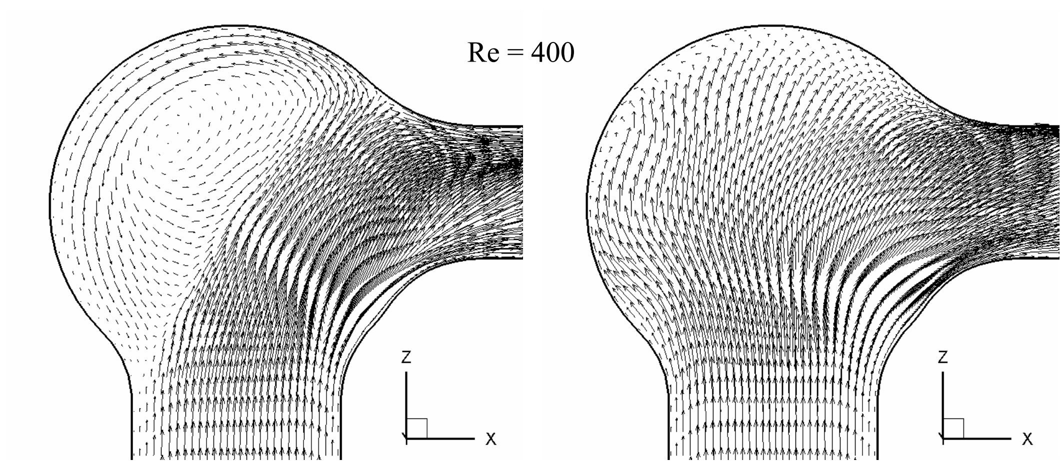


Figure 5. Instantaneous flow maps at the *x*-*z* meridional plane of the spherical bulge for $Re = 400$, depicting small-amplitude oscillations (left) and a bursting event (right).

## Conclusions

Unsteady numerical simulations of the flow through a spherical bulge in a 90° asymmetrical bend have been carried out for Reynolds number in the range 100-400. Preliminary results obtained employing a coarse discretization of the physical domain have shown that the flow reaches asymptotically steady solutions for Reynolds numbers up to 300. By contrast, the flow behavior at a Reynolds number of 400 has shown to be characterized by long transients of small-amplitude, irregular oscillations, which are suddenly disrupted by short periods of large-amplitude bursts. However, such intermittent behavior exhibits an organized pattern, as the bursts occur at an approximately constant non-dimensional frequency value of 0.018. The observed unsteadiness is accompanied by symmetry-breaking of the flow topology inside the bulge.

## References

1 Rockwell, D. and Naudascher, E. (1978): "Review – Self-Sustained Oscillations of Flows Past Cavities", *ASME Journal of Fluids Engineering*, Vol. 100, pp. 152-165.

2 Pereira, J. C. F. and Sousa, J. M. M. (1993): "Finite Volume Calculations of Self-Sustained Oscillations in a Grooved Channel", *Journal of Computational Physics*, Vol. 106, pp. 19-29.

3 Pereira, J. C. F. and Sousa, J. M. M. (1995): "Experimental and Numerical Investigation of Flow Oscillations in a Rectangular Cavity", *ASME Journal of Fluids Engineering*, Vol. 117, pp. 68-74.

4 Drazin, P. G. (1999): "Flow through a Diverging Channel: Instability and Bifurcation", *Fluid Dynamics Research*, Vol. 24, pp. 321-327.

5 Fearn, R. M., Mullin, T. and Cliffe, K. A. (1990): "Nonlinear Flow Phenomena in a Symmetric Sudden Expansion", *Journal of Fluid Mechanics*, Vol. 211, pp. 595-608.

6 Sobey, I. J. and Drazin, P. G. (1986): "Bifurcations of Two-Dimensional Channel Flows", *Journal of Fluid Mechanics*, Vol. 171, pp. 263-287.

7 Liou, T. M. and Liou, S. N. (1999): "A Review on *In Vitro* Studies of Hemodynamic Characteristics in Terminal and Lateral Aneurysm Models", *Proceedings of the National Science Council ROC (B)*, Vol. 23, pp. 133-148.

8 Yip, T. H. and Yu, S. C. M. (2001): "Cyclic Transition to Turbulence in Rigid Abdominal Aortic Aneurysm Models", *Fluid Dynamics Research*, Vol. 29, pp. 81-113.

9 Butty, V. D., Gudjonsson, K., Buchel, P., Makhijani, V. B., Ventikos, Y. and Poulikakos, D. (2002): "Residence Times and Basins of Attraction for a Realistic Right Internal Carotid Artery with Two Aneurysms", *Biorheology*, Vol. 39, pp. 387-393.

10 Pereira, J. C. F. and Sousa, J. M. M. (1999): "Confined Vortex Breakdown Generated by a Rotating Cone", *Journal of Fluid Mechanics*, Vol. 385, pp. 287-323.

11 Lichtenberg, A. J. and Lieberman, M. A. (1992): *Regular and Chaotic Dynamics*, Springer.

12 Mendes, P. J., Pinto, J. F. and Sousa, J. M. M. (2004): "LDA measurements of flow velocity through a standard analyser used for quality control of medical aerosol products", 12th International Symposium on Applications of Laser Techniques to Fluid Mechanics, Lisbon, 12-15 July (to be presented).